

A network of genetic repression and derepression specifies projection fates in the developing neocortex

Karpagam Srinivasan^{a,1}, Dino P. Leone^a, Rosalie K. Bateson^a, Gergana Dobreva^b, Yoshinori Kohwi^c, Terumi Kohwi-Shigematsu^c, Rudolf Grosschedl^b, and Susan K. McConnell^{a,2}

^aDepartment of Biology, Stanford University, Stanford, CA 94305; ^bMax-Planck Institute of Immunobiology and Epigenetics, 79108 Freiburg, Germany; and ^cLawrence Berkeley National Laboratory, Berkeley, CA 94720

This contribution is part of the special series of Inaugural Articles by members of the National Academy of Sciences elected in 2011.

Contributed by Susan K. McConnell, September 28, 2012 (sent for review August 24, 2012)

Neurons within each layer in the mammalian cortex have stereotypic projections. Four genes—*Fezf2*, *Ctip2*, *Tbr1*, and *Satb2*—regulate these projection identities. These genes also interact with each other, and it is unclear how these interactions shape the final projection identity. Here we show, by generating double mutants of *Fezf2*, *Ctip2*, and *Satb2*, that cortical neurons deploy a complex genetic switch that uses mutual repression to produce subcortical or callosal projections. We discovered that *Tbr1*, *EphA4*, and *Unc5H3* are critical downstream targets of *Satb2* in callosal fate specification. This represents a unique role for *Tbr1*, implicated previously in specifying corticothalamic projections. We further show that *Tbr1* expression is dually regulated by *Satb2* and *Ctip2* in layers 2–5. Finally, we show that *Satb2* and *Fezf2* regulate two disease-related genes, *Auts2* (Autistic Susceptibility Gene2) and *Bhlhb5* (mutated in Hereditary Spastic Paraplegia), providing a molecular handle to investigate circuit disorders in neurodevelopmental diseases.

cell fate | cerebral cortex | axon guidance | transcription factor

Cortical neurons project to specific targets located locally within the cortex or in distant subcortical regions, depending on the neuron's birthdate and laminar position. Neurons in layer 5 project subcortically to targets that include the spinal cord, whereas neurons in layers 2/3 typically project corticocortically, including across the corpus callosum (CC) (1–3). Four key genes—*Fezf2*, *Ctip2*, *Tbr1*, and *Satb2*—are involved in specifying projection neuron identity (3–7). *Fezf2* and *Ctip2* regulate the identities of layer 5 subcerebral projection neurons (SCPNs), whereas *Satb2* regulates the fate of callosally projecting neurons (Fig. 10). Without *Fezf2*, SCPNs up-regulate *Satb2*, switch fate, and extend axons across the CC (8), suggesting that *Fezf2* represses *Satb2* and the acquisition of a callosal identity. Conversely, without *Satb2*, callosal neurons up-regulate *Ctip2* (but not *Fezf2*) and project subcortically (9, 10). Biochemical experiments revealed that *Satb2* binds to and represses the *Ctip2* locus (9) but have not ascertained whether the fate switch in *Satb2* mutant neurons is a direct consequence of *Ctip2* upregulation.

Layer 6 corticothalamic neurons and layer 5 SCPNs show a similar mutual repression between *Tbr1* (layer 6) and *Fezf2* (layer 5) (3–7). Deep layer neurons in *Tbr1*^{-/-} mice up-regulate *Fezf2* and project inappropriately to the pons, while *Fezf2*^{-/-} neurons up-regulate *Tbr1* and form thalamic projections (Fig. 10). Thus, *Fezf2* represses both *Tbr1* and *Satb2*, which repress corticothalamic and callosal fates in SCPNs. The nature of these repressive interactions, however, is unknown. Here we analyze mice bearing mutations in *Fezf2*, *Ctip2*, and *Satb2* to examine the genetic relationships between these pathways. Using in vivo electroporation to rescue callosal axons in *Satb2* mutants, we identified downstream targets of *Satb2* that play key roles in the formation of callosal projections.

In this study, data obtained from double knockouts of *Satb2*, *Fezf2*, and *Ctip2* (together with previously published data) provide evidence for a genetic model of cortical projection neuron fate determination during early corticogenesis (Fig. S1A). In *Fezf2*-expressing neurons, expression of *Tbr1* and *Satb2* is repressed,

which results in a suppression of corticothalamic and callosal fates, respectively, and axon extension along the corticospinal tract (CST). *Fezf2* mutant neurons fail to repress *Satb2* and *Tbr1*, thus their axons cross the CC and/or innervate the thalamus inappropriately.

In callosal projection neurons, *Satb2* represses the expression of *Ctip2* and *Bhlhb5*, leading to a repression of subcerebral fates. Interestingly, we found that *Satb2* promotes *Tbr1* expression in upper layer callosal neurons, and *Tbr1* expression in these neurons is required for callosal specification (not corticothalamic specification). Our data suggest that the projection fates of deep layer and upper layer cortical pyramidal neurons are specified by complex and mutually inhibitory genetic interactions between postmitotic determinants during late embryonic development.

Results

Visualization of Callosal and Subcortical Axonal Connections in *Satb2* and *Fezf2* Mutants. We visualized callosal axons using mice in which *LacZ* was targeted to the *Satb2* locus (9). In embryonic day (E) 18.5 control *Satb2*^{LacZ/+} mice, β-galactosidase positive (β-gal⁺) axons cross the CC and form corticocortical connections (Fig. S2 B and O) but do not extend subcortically (Fig. S2 A and O). As shown previously, β-gal⁺ axons in E18.5 *Satb2*^{LacZ/LacZ} mutants fail to cross the CC and instead descend subcortically through the striatum and along the cerebral peduncle and to the thalamus (Fig. S2 C, D, and P). Thus, without *Satb2*, callosal neurons seem to be respecified as subcortical projection neurons (9, 10). *Satb2*^{LacZ/LacZ} mice die within a few hours after birth, which precludes the analysis of axonal connectivity at postnatal stages. Here we also use mice bearing a conditional allele of *Satb2* (*Satb2*^{lox/lox}, generated in the laboratory of R.G.) bred with mice that express Cre recombinase under the *Emx1* promoter (*Emx1-Cre*) to produce viable, cortex-specific *Satb2* knockouts. Mice carrying *Emx1-Cre* also carried the *Satb2*^{LacZ} allele, enabling us to generate conditional *Satb2*^{LacZ/lox}; *Emx1-Cre* knockout mice in which the axons of neurons that normally express *Satb2* neurons are marked by β-gal (Fig. 1B, D–G). A detailed description of *Satb2* conditional knockout mice is in preparation.

The insertion of a placental alkaline phosphatase (PLAP) cassette into the *Fezf2* locus (11) enabled us to visualize the projections of deep layer cells that normally express *Fezf2*. PLAP⁺ axons in *Fezf2*^{PLAP/+} controls are observed in the pyramidal tract (Fig. 2 A and E) and thalamus (Fig. S4I), whereas labeled axons are absent from the CC, as previously described (8, 11). At P0, PLAP⁺ axons

Author contributions: K.S. and S.K.M. designed research; K.S., D.P.L., and R.K.B. performed research; K.S., D.P.L., and S.K.M. analyzed data; G.D., Y.K., T.K.-S., and R.G. contributed new reagents/analytic tools; K.S., D.P.L., and S.K.M. wrote the paper; Y.K. and T.K.-S. provided technical advice with ChIP experiments.

The authors declare no conflict of interest.

¹Present address: Neurodegeneration Laboratories, Department of Neuroscience, Genentech, South San Francisco, CA 94080.

²To whom correspondence should be addressed. E-mail: suemcc@stanford.edu.

This article contains supporting information online at www.pnas.org/lookup/suppl/doi:10.1073/pnas.1216793109/-DCSupplemental.

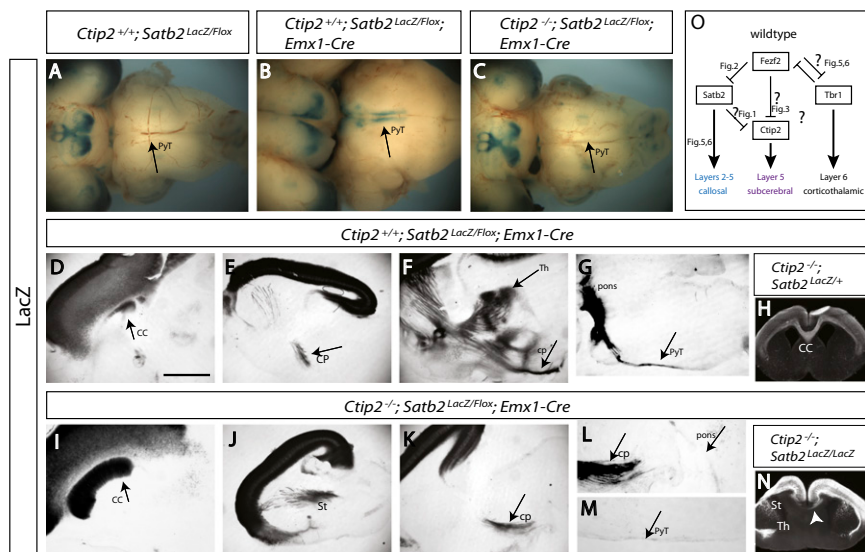


Fig. 1. Loss of *Ctip2* partially rescues callosal projections in *Satb2* mutant neurons. (A–C) LacZ staining of P0 whole-mount brains (ventral view) reveals aberrant β -gal⁺ axons (blue) in the pyramidal tract (arrow) in *Satb2*^{LacZ/Flox}; *Emx1*-Cre mutants (B) but not in control mice (A) or *Ctip2*^{-/-}; *Satb2*^{LacZ/Flox}; *Emx1*-Cre double knockouts (C). (D) The majority of β -gal⁺ callosal axons in *Satb2* conditional mutants fail to project across the CC at P0. (E and F) Instead, these axons project subcortically into the cerebral peduncle (cp) and thalamus (Th). (G) A small number of β -gal⁺ axons are seen in the pyramidal tract (PyT). (H) Coronal sections of *Ctip2*^{-/-}; *Satb2*^{LacZ/+} mice reveal β -gal⁺ axons crossing normally at the CC. (I and N) β -gal⁺ callosal axons in *Satb2*; *Ctip2* double mutants are seen at the CC (arrow) at P0. Defasciculated β -gal⁺ axons also descend subcortically into the striatum (J), along the cerebral peduncle (K and L) but not to the level of the pyramidal tract (M). (O) Model outlining genetic interactions between *Fezf2*, *Ctip2*, *Satb2*, and *Tbr1* described previously during cortical projection neuron fate specification. Question marks denote interactions that are not clearly understood. (Scale bar in D, 200 μ m.)

descend subcortically and branch toward the thalamus (Fig. S3B) and cerebral peduncle (Fig. S3B) but do not extend past the pons. At postnatal day (P) 4, *Fezf2*^{PLAP/PLAP} mutants show a striking reduction in the number of PLAP⁺ axons that extend into the pyramidal tract at the level of the hindbrain (Fig. 2B and F). In addition, a subset of PLAP⁺ axons cross the CC (Fig. 2I and J), consistent with the interpretation (Fig. S1B) that at least some neurons that normally express *Fezf2* acquire a callosal identity in the absence of *Fezf2*, possibly owing to acquisition of *Satb2* expression (8).

Interactions Between *Fezf2* and *Satb2* in the Regulation of Subcortical Identity. We tested the role of *Satb2* in the respecification of deep layer fates by generating *Fezf2*; *Satb2* double mutants, predicting that PLAP⁺ axons should fail to extend across the CC. Indeed, analysis of *Fezf2*^{PLAP/PLAP}; *Satb2*^{LacZ/LacZ} mice revealed a loss of PLAP⁺ axons in the CC at P0 (Fig. 2K), providing strong evidence that the acquisition of a callosal fate of *Fezf2* mutant neurons is due to up-regulation of *Satb2*. Visualization of PLAP⁺ axons in the sagittal plane showed axons projecting subcortically through the striatum and exiting through two branches, one directed toward the thalamus (Fig. S3B and C) and the other into the cerebral peduncle (Fig. S3B and C), although the latter axons

fail to reach the hindbrain (Fig. S3B, asterisk). The β -gal⁺ axons of *Satb2*-expressing neurons in the same section follow a similar tract, although they extend past the peduncle toward the pons (Fig. S3A and C) but fail to reach it.

This difference in the extent of subcortical innervation by PLAP⁺ vs. β -gal⁺ axons suggested that loss of *Satb2* might affect the formation of subcortical projections by layer 5 neurons, which normally express *Fezf2* but not *Satb2*. To ascertain whether mice lacking both *Fezf2* and *Satb2* simply show a developmental delay in the growth of subcortical projections, we analyzed PLAP staining at P4 in *Fezf2*^{PLAP/PLAP}; *Satb2*^{LacZ/Flox}; *Emx1*-Cre double mutants. Whole mounts revealed a complete loss of PLAP⁺ axons in the pyramidal tract (Fig. 2D), whereas littermates lacking only *Fezf2* retain some PLAP staining of pyramidal tract axons (Fig. 2B). These data suggest the surprising possibility that *Satb2* plays a role in the normal targeting of SCPNs.

If this hypothesis is correct, subcortical axons in *Satb2* mutants should display defects in their projection patterns. We therefore examined the pattern of PLAP labeling in mice lacking *Satb2* and carrying one copy of the *Fezf2*^{PLAP} allele. In *Fezf2*^{PLAP/+}; *Satb2*^{LacZ/LacZ} mutants at E18, a thin tract of PLAP⁺ axons extends subcortically toward the cerebral peduncle but does not reach

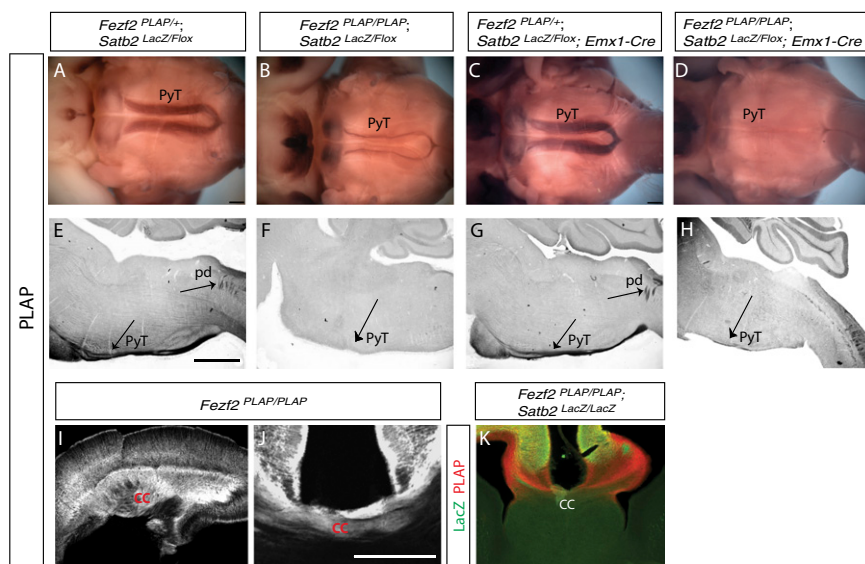


Fig. 2. Loss of *Satb2* does not rescue PLAP⁺ axons in *Fezf2*^{PLAP/PLAP} mutants. (A–D) Whole-mount PLAP staining of *Fezf2*^{PLAP/+} heterozygous mice (A) and *Satb2* conditional mutants (C) reveals that PLAP⁺ axons extend into the pyramidal tract (PyT). (B) *Fezf2*^{PLAP/PLAP} mutants show a dramatic decrease in PLAP staining in the pyramidal tract. (D) In *Fezf2*^{PLAP/PLAP}; *Satb2*^{LacZ/Flox}; *Emx1*-Cre double mutants, there is a complete loss of PLAP staining in the pyramidal tract. (E–H) PLAP staining of sagittal sections from the brains shown in A–D. PLAP⁺ axons in heterozygous *Fezf2*^{PLAP/+} controls (E) and *Satb2*^{LacZ/Flox}; *Emx1*-Cre mutants (G) project subcortically through the pyramidal tract (PyT) and pyramidal decussation (pd). (H) PLAP⁺ axons in *Fezf2*^{PLAP/PLAP}; *Satb2*^{LacZ/Flox}; *Emx1*-Cre double mutants fail to enter the pyramidal tract. (Scale bar, 200 μ m.) (I and J) In *Fezf2* mutants, PLAP⁺ axons are present in the CC in both sagittal (I) and coronal (J) sections. (K) Both PLAP⁺ (red) and β -gal⁺ (green) axons fail to cross the CC in *Fezf2*^{PLAP/PLAP}; *Satb2*^{LacZ/Flox}; *Emx1*-Cre double mutants. (Scale bars, 200 μ m.)

the pyramidal tract (Fig. S4F). In conditional *Satb2* mutants (*Fezf2^{PLAP/+};Satb2^{lox/lox};Emx1-Cre*) at P4, PLAP⁺ axons reach past the pons to the pyramidal decussation (Fig. 2 C and G), but the axons fail to enter the spinal cord (Fig. S4 G and H). To determine whether this reflects a failure of corticospinal innervation or a developmental delay, we immunostained conditional *Satb2* knockouts at P21 (when PLAP can no longer be detected in our animals) using antibodies against protein kinase C γ (PKC γ), which labels the CST (12). These studies revealed a complete loss of PKC γ staining in the spinal cord, consistent with a loss of corticospinal connections.

These analyses of PLAP⁺ axons in *Satb2* mutants yield the unexpected conclusion that *Satb2* is required for the normal growth of subcerebral axons to their targets in the spinal cord. How might *Satb2* exert this effect? One possibility is that *Satb2* plays a non-cell autonomous role in subcerebral neurons development. However, our prior studies have shown that *Satb2* and *Ctip2* are normally coexpressed in layer 5 neurons during a brief period early in corticogenesis (E13.5–E14) (9). Thus, although *Satb2* may be expressed only transiently in subcerebral neurons, this window of expression may play a critical role in regulating the expression of key genes such as axon guidance molecules. For example, *Satb2* mutants show reduced expression of *Unc5H3*, a well-characterized axonal guidance receptor (9). In *Unc5H3* mutants, subcerebral axons fail to descend past the decussation into the spinal cord (13), raising the possibility that *Satb2* knockouts display a similar phenotype due to reduced expression of *Unc5H3*. An alternative possibility is that *Satb2* may play a non-cell autonomous role in guiding subcerebral axons to the spinal cord. For example, *Satb2* is expressed in interneurons and in the spinal cord, and it is possible that this expression is required for corticospinal axon guidance. However, in our analyses of conditional *Satb2* mutants (in which expression in interneurons is maintained), we observe the same phenotype as the straight *Satb2* knockouts. Therefore, it is unlikely that *Satb2* expression in interneurons is essential for guiding subcerebral axons to the spinal cord.

Genetic Interactions Between *Satb2* and *Ctip2* in the Formation of Subcerebral Projections. Previous studies using *Ctip2* knockout mice suggest that *Ctip2* is required for the normal formation of subcerebral projections, which are defasciculated and terminate prematurely in these mutants (1). *Ctip2*^{-/-} mice do not carry a reporter allele (1), therefore analysis of axonal projections in these animals has been limited to using dye tracers. Because *Fezf2* expression is not altered in *Ctip2*^{-/-} mutants (Fig. S4A) and because *Fezf2* and *Ctip2* seem to be coexpressed in deep layer neurons (8, 14), we used *Fezf2^{PLAP}* as a marker for subcerebral projections. As expected, PLAP⁺ axons in *Ctip2^{+/-}*;

Fezf2^{PLAP/+} heterozygous brains extend subcortically through the striatum; some extend into the thalamus, whereas others are present in the cerebral peduncle (Fig. S4I) and pyramidal tract (Fig. S4J). In *Ctip2*^{-/-} mutants carrying a *Fezf2^{PLAP}* allele, defasciculated PLAP⁺ axons pass through the striatum and extend into the thalamus or cerebral peduncle (Fig. S4K) but do not reach the pons (Fig. S4K, Inset). This pattern is similar to that seen by dye-labeling subcerebral axons in *Ctip2* mutants (1).

Our model of the genetic interactions that confer projection neuron fates predicts that in the absence of both *Ctip2* and *Satb2* (Fig. S1F), PLAP⁺ SCPNs should form projections similar to those seen in *Ctip2* single mutants (Fig. S1C). We used PLAP staining to trace the projections of these neurons in *Ctip2;Satb2* double mutants (*Ctip2*^{-/-};*Fezf2^{PLAP/+}*;*Satb2^{LacZ/lox}*;*Emx1-Cre*) (Fig. S3 D–F). PLAP⁺ axons (in red) are absent from the CC and can be seen subcortically at the level of cerebral peduncle (Fig. S3E). PLAP⁺ axons are absent from the thalamus in sagittal sections (Fig. S3D, asterisk), consistent with the prediction (Fig. S1F) that layer 5 neurons that lose both *Ctip2* and *Satb2* expression will express only low levels of *Tbr1*. These neurons, however, continue to express *Fezf2* and *Bhlhb5*, both of which impart a subcortical identity to the neurons, as evidenced by PLAP⁺ axons in the cerebral peduncle. However, without *Ctip2*, these neurons are unable project past the pons.

Loss of *Satb2* Rescues *Ctip2* Expression in *Fezf2^{PLAP/PLAP}* Neurons. *Ctip2* expression is down-regulated in layer 5 of *Fezf2* mutants (11) (Fig. 3B), suggesting that *Ctip2* may be a downstream target of *Fezf2*. However, because *Fezf2* normally represses *Satb2* genetically (8), and *Satb2*, in turn, represses *Ctip2* (9) (Fig. 3C), it is possible that the loss of *Ctip2* expression in *Fezf2^{PLAP/PLAP}* mutant neurons is an indirect consequence of the up-regulation of *Satb2*, rather than the result of direct transcriptional control of *Ctip2* by *Fezf2*. If the regulation is indirect via *Satb2*, we predict that *Ctip2* expression will be restored in layer 5 neurons in *Fezf2^{PLAP/PLAP}*;*Satb2^{LacZ/lox}*;*Emx1-Cre* double mutants (Fig. S1E). Indeed, we do observe strong *Ctip2* expression in layer 5 neurons in double mutants (Fig. 3D), suggesting that *Fezf2* regulates *Ctip2* indirectly by repressing *Satb2*.

We counted the number of *Ctip2*-expressing cells across the cortical layers, first in single knockouts for *Fezf2* or *Satb2*. In layer 6 (Fig. 3G), the number of *Ctip2*⁺ cells increased from 29% ± 1.5% in control mice to 39% ± 1.8% (*P* < 0.006) in *Fezf2* mutants and 47% ± 5.4% (*P* < 0.01) in *Satb2* conditional mutants. In layer 5, the total number of *Ctip2*⁺ cells decreased in *Fezf2* mutants (57% ± 7% in controls vs. 10% ± 3% in mutants, *P* < 0.001) but increased to 83% ± 4% in *Satb2* mutants (*P* < 0.01) (Fig. 3F). This suggests that the loss of *Ctip2* in layer 5 of *Fezf2* mutants might be due to the acquisition of *Satb2* expression

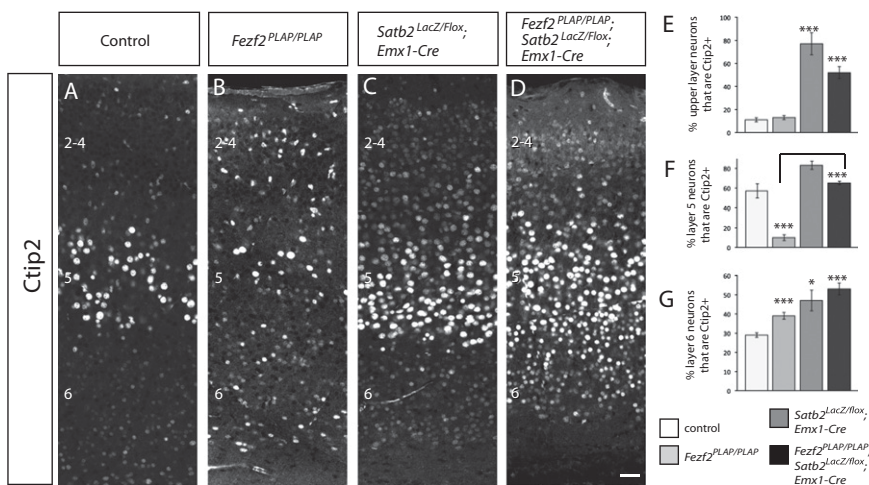


Fig. 3. *Ctip2* expression is restored in layer 5 neurons of *Fezf2^{PLAP/PLAP}*;*Satb2^{LacZ/lox}*;*Emx1-Cre* double mutants. (A) In WT mice, the expression of *Ctip2* protein is highest in layer 5 neurons, moderate in layer 6, and largely absent from the upper layers (2–4). (B) *Fezf2* mutants show a severe reduction of *Ctip2* expression in layer 5, whereas expression in layer 6 is increased. (C) *Satb2* mutant mice show increased *Ctip2* expression in layer 5, 6, and the upper layers. (D) *Ctip2* expression is rescued in layer 5 of *Fezf2^{PLAP/PLAP}*;*Satb2^{LacZ/lox}*;*Emx1-Cre* double mutants. (A–D) Each panel is a composite of tiled confocal images to form the full figure. (Scale bar, 50 μ m.) (E–G) Graphs depict the percentages of *Ctip2*⁺ neurons in the upper layers (E), layer 5 (F), and layer 6 (G) in various genotypes. Error bars are average ± SEM (*n* = 3 different animals). Confidence levels were calculated using a *t* test (**P* < 0.5; ***P* < 0.05; ****P* < 0.005, relative to controls).

(Fig. S4C) (8). *Satb2* also represses *Ctip2* expression in the upper layers, as evidenced by the dramatic increase in *Ctip2*⁺ cells from 11% ± 1.7% in controls to 77% ± 9.5% ($P < 0.05$) in *Satb2* mutants (Fig. 3E).

To ascertain whether *Ctip2* is regulated directly by *Fezf2* or indirectly by *Satb2*, we counted the numbers of *Ctip2*⁺ cells in *Satb2*^{LacZ/flox}; *Fezf2*^{PLAP/PLAP}; *Emx1-Cre* double mutants. The loss of *Ctip2* expression in layer 5 neurons of *Fezf2*^{PLAP/PLAP} mutants (10% ± 3%) is rescued in double mutants (65% ± 1.8%; $P < 0.0005$) (Fig. 3F), providing strong evidence that at this stage in development, *Fezf2* regulates *Ctip2* indirectly by repressing *Satb2*.

Satb2 Regulates Bhlhb5 Expression. Knowing that *Fezf2* regulates *Ctip2* indirectly by repressing *Satb2*, we asked whether other genes important for SCPN identity, such as *Bhlhb5*, are regulated similarly. *Bhlhb5* is expressed by *Ctip2*⁺ neurons in layer 5 as well as in neurons in layers 2/3 (12). *Bhlhb5* functions as an area-specific transcription factor that regulates the postmitotic acquisition of area-specific identities. In caudal motor cortex, *Bhlhb5* null mice exhibit anomalous differentiation of corticospinal motor neurons, accompanied by failure of CST formation (12). The axons stop at the base of the pons and fail to enter the pyramidal tract (similar to *Ctip2*^{-/-} mutant axons at P0).

To ascertain whether *Fezf2* regulates the expression of *Bhlhb5*, we immunostained *Fezf2*^{PLAP/PLAP} brains for *Bhlhb5* protein. The number of *Bhlhb5*⁺ cells is significantly reduced in layer 5 of *Fezf2* mutants (Fig. 4C) relative to controls (Fig. 4A) (64% ± 3% in controls to 12% ± 4.5% in mutants; $P < 0.005$). If this is due to the expansion of *Satb2* expression in *Fezf2* mutants (Fig. S4C), *Bhlhb5* expression should be rescued in layer 5 neurons that lack *Satb2*. Indeed, the number of *Bhlhb5*⁺ cells in layer 5 in P4 mice is restored to 49% ± 3.9% in double mutants (*Fezf2*^{PLAP/PLAP}; *Satb2*^{LacZ/flox}; *Emx1-Cre*) (Fig. 4D and H; $P < 0.001$ compared with *Fezf2* single mutants). These data suggest that *Fezf2* regulates *Bhlhb5* expression in layer 5 indirectly by repressing *Satb2*, and that *Satb2* functions as a repressor of *Bhlhb5*. Consistent with the latter interpretation, upper layer neurons of *Satb2* mutant mice exhibited a robust increase in both the number of *Bhlhb5*⁺ neurons in layers 2–4 (Fig. 4G; control: 28% ± 7.8%; *Satb2*^{LacZ/flox}; *Emx1-Cre* conditional mutants, 63% ±

2.4%, $P < 0.005$) (Fig. 4B). Because *Bhlhb5* is normally expressed by upper layer neurons, this regulation by *Satb2* is unlikely to represent an on/off switch, but rather a mechanism that regulates the timing and levels of *Bhlhb5* expression. Indeed, *Bhlhb5* expression seems unchanged in the upper layers of *Satb2* mutants at E18; the change is evident only by P4. This suggests that *Satb2* likely regulates the timing of down-regulation of *Bhlhb5* in upper layer neurons rather than an on/off switch for *Bhlhb5* expression itself. It is also possible that *Bhlhb5* is regulated by other factors expressed by upper layer neurons and that the final expression pattern reflects the action of multiple regulatory pathways.

Finally, we found that normal *Bhlhb5* expression in some deep layer neurons also requires *Ctip2*. The percentage of *Bhlhb5*⁺ neurons in layer 6 is increased significantly in *Ctip2*^{-/-} mice (Fig. 4E and I; control: 9% ± 4%, mutants: 70% ± 4.5%; $P < 0.0005$). However, in contrast to the severe reduction of *Bhlhb5*⁺ neurons in layer 5 of *Fezf2* mutants, there is no significant change in the percentage of layer 5 neurons that express *Bhlhb5* in *Ctip2* mutants. Because *Satb2* expression seems to be unaltered in the absence of *Ctip2*, these data are consistent with the interpretation that *Satb2* is a primary regulator of *Bhlhb5* in layer 5.

To determine whether high levels of *Bhlhb5* expression are sufficient to direct axons toward subcortical targets, we coelectroporated expression constructs encoding *Bhlhb5* and GFP into WT embryos at E15.5, a time when upper layer neurons are being generated. As expected, GFP labeled neurons are present in the upper layers in control (GFP only) (Fig. 4J) and *Bhlhb5* plus GFP (Fig. 4M) electroporated brains. At P4, in control brains, GFP-labeled axons were confined to the ipsilateral and contralateral cerebral cortices (Fig. 4J), and no GFP⁺ axons can be observed subcortically in the striatum (Fig. 4K) or at the level of the cerebral peduncle. In these brains, GFP⁺ axons can be seen at the CC (Fig. 4L), indicating that as expected, electroporated neurons from upper layers may be sending the axons across the midline to the contralateral hemisphere. In contrast, the GFP⁺ axons of *Bhlhb5*-electroporated neurons extend beyond the striatal boundary into the internal capsule (Fig. 4N) and toward the cerebral peduncle (Fig. 4P, arrow). We do observe some GFP⁺ axons in the CC (Fig. 4O), which is probably because not all GFP⁺ cells express *bhlhb5*. These results suggest

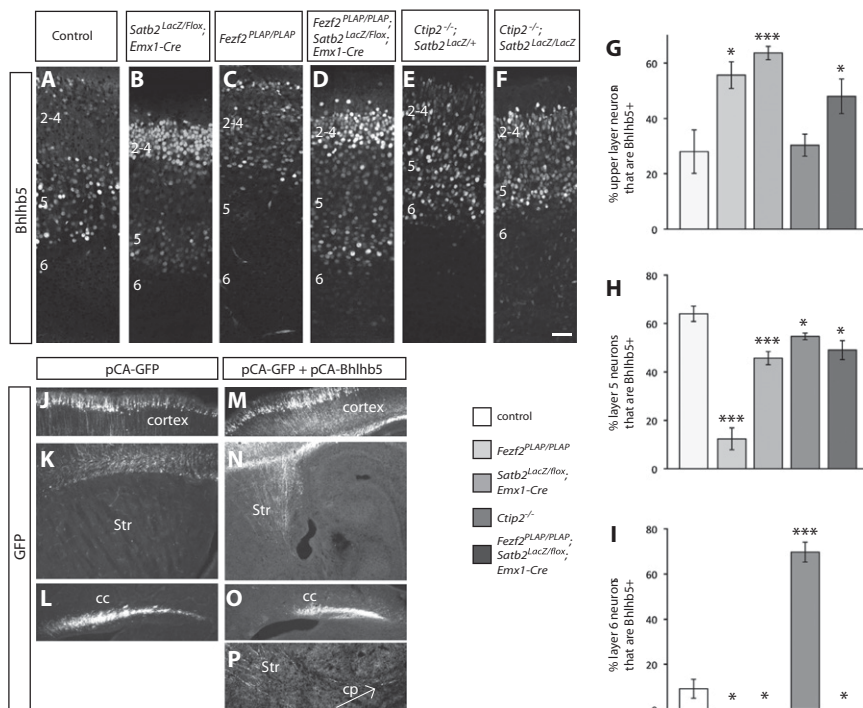


Fig. 4. *Satb2* regulates *Bhlhb5* expression in a layer-specific manner. (A) In controls, *Bhlhb5* protein is expressed at high levels in layer 5 neurons and at low to moderate levels in the upper layers. (B) In *Satb2*^{LacZ/flox}; *Emx1-Cre* mutants, *Bhlhb5* expression is significantly reduced in layer 5. (C) Expression in both layers 5 and 6 is decreased in the *Fezf2* mutant cortex. (D) *Bhlhb5* expression in layer 5 is rescued in *Fezf2*^{PLAP/PLAP}; *Satb2*^{LacZ/flox}; *Emx1-Cre* double mutants. (E and F) In *Ctip2*^{-/-} mutants (E) and *Ctip2*^{-/-}; *Satb2*^{LacZ/LacZ} double mutants (F), expression is increased in both layer 5 and the upper layers. (A–F) Each panel is a composite of tiled confocal images to form the full figure. (Scale bar, 50 μ m.) (G–I) Graphs depict the percentages of *Bhlhb5*⁺ neurons in different genotypes in different cortical layers. Error bars depict average \pm SEM ($n = 3$ different animals). Confidence levels were calculated using a t test (* $P < 0.5$; ** $P < 0.05$; *** $P < 0.005$, relative to controls). (J–P) Ectopic overexpression of *Bhlhb5* in upper layer neurons of WT animals can redirect their axons subcortically. (J–L) Sagittal sections of P4 control brains electroporated with GFP at E15 (when upper layer neurons are born) show (J) GFP⁺ neurons in the upper layers; (K) no GFP⁺ axons in the ipsilateral striatum (Str); and (L) GFP⁺ axons in the CC. (M–P) Sagittal sections of P4 brains electroporated with *Bhlhb5* and GFP at E15 show (M) GFP⁺ neurons in the upper layers; and (N) robust GFP⁺ tracts extending through the striatum (Str) and (P) toward the cerebral peduncle (cp, arrows). (O) GFP⁺ axons are also observed in the CC. (Scale bar, 50 μ m.)

that *Bhlhb5* by itself has a limited but real potential to direct axons to subcortical targets, less robust than that of *Ctip2* (8) and similar to that observed after *Sox5* electroporation at E15.5 (15, 16).

***Fezf2*, *Ctip2*, and *Satb2* Regulate *Tbr1* Expression in a Layer-Specific Manner.** *Fezf2* and *Tbr1* play important antagonistic roles in the regulation of layer 6 axons to the thalamus. *Tbr1* mutants show a loss of corticothalamic projections, whereas *Fezf2* mutants show a striking increase in thalamic innervation, most likely due to increased expression of *Tbr1* (5, 7). In controls (Fig. 5A), the highest level of *Tbr1* expression is observed in layer 6, with lower levels in layer 5 and scattered cells labeled in the upper layers. Consistent with previously published reports (5, 7), we found that the number of *Tbr1*⁺ neurons increases significantly in layer 5 and upper layer neurons of *Fezf2* mutants (Fig. 5E, G, and H) (control layer 5: 22% ± 4.7%, mutant layer 5: 54% ± 8.9% *P* < 0.05; control upper layers: 23% ± 7%, mutant upper layers: 43% ± 3%; *P* < 0.05) but is not significantly changed in layer 6 (Fig. 5I). *Fezf2* mutants also show a robust band of PLAP fibers entering (Fig. 6F) and innervating the anterior thalamus (Fig. 6M), which might be a consequence of increased *Tbr1* expression in layer 5. Interestingly, *Ctip2*^{-/-} mutants also show a significant increase in the number of *Tbr1*⁺ layer 5 neurons (most obviously in layer 5b) (Fig. 5C and H; mutants: 54% ± 1.79%, *P* < 0.002), along with increased PLAP labeling in the thalamus (Fig. 6J and O), suggesting that *Ctip2* represses *Tbr1*. Because *Ctip2* is genetically downstream of *Fezf2* and because the increase in *Tbr1* expression is similar in *Fezf2* and *Ctip2* mutants, it is possible that *Fezf2* regulates *Tbr1* expression indirectly via *Ctip2*.

The genetic relationship between *Satb2* and *Ctip2* led us to predict that *Tbr1* expression should decrease in *Satb2* mutants, owing to the up-regulation of *Ctip2*. The number of *Tbr1*⁺ neurons in layer 5 of *Satb2* mutants is significantly decreased (Fig. 5B and H; 3% ± 1.2%, *P* < 0.004) relative to controls, and PLAP innervation of the thalamus is reduced in *Satb2* mutants (Fig. 6D and L). Interestingly, in *Fezf2*^{PLAP/PLAP};*Satb2*^{LacZ/LacZ} double knockouts, we observe PLAP⁺ axons in the thalamus, although the extent of innervation qualitatively seems to be less than in *Fezf2* mutants but more than in *Satb2* mutants (Fig. 6G, H, and N). Indeed, *Tbr1* expression in layer 5 neurons of double knockouts is significantly increased compared with *Satb2* mutants (*Satb2*^{LacZ/LacZ}; 3% ± 1.2%; *Fezf2*^{PLAP/PLAP};*Satb2*^{LacZ/LacZ} double mutants: 12% ± 1.2%; *P* < 0.02). *Satb2* mutants also show a nearly complete loss of *Tbr1*⁺ neurons in the upper layers (Fig. 5G; control: 23% ± 7.2%, mutant: 4% ± 0.3%; *P* < 0.01). There is a small but not significant change in layer 6, where *Satb2*

expression is relatively low (Fig. 5I; control: 63% ± 7.8%, mutant: 49% ± 5.4%; *P* < 0.1). Taken together, these data provide evidence that *Tbr1* is regulated negatively by *Ctip2* (and *Fezf2*).

Counting the number of *Tbr1*⁺ neurons in layer 5 of *Ctip2*^{-/-}; *Satb2*^{LacZ/Flox}; *Emx1-Cre* double knockouts yielded a surprising result. Although there are more *Tbr1*⁺ cells in layer 5 of the double knockouts compared with *Satb2* single mutants (Fig. 5H; 8% ± 1.8% in double mutants and 3% ± 1.2% in *Satb2* mutants, *P* < 0.005), the numbers are neither restored to WT levels (22% ± 4.8%) nor to that of *Ctip2* single mutants (54% ± 1.8%), suggesting that *Ctip2* is not the sole regulator of *Tbr1* expression and that *Satb2* might positively regulate *Tbr1*. Moreover, *Ctip2*^{-/-}; *Satb2*^{LacZ/Flox}; *Emx1-Cre* double knockouts fail to show a restoration of *Tbr1* expression in the upper layers (Fig. 5D and G), further providing evidence that *Satb2* is required for the expression of *Tbr1* in these neurons (independent of *Ctip2*). These studies suggest the possibility that *Satb2* might bind directly to the *Tbr1* genomic locus and promote its expression.

***Satb2* Binds Directly to the *Tbr1* Genomic Locus.** To determine whether *Satb2* can bind directly to the *Tbr1* locus, we identified three so-called MAR sites (Matrix Attachment Sequences) in the *Tbr1* locus that have the potential to serve as *Satb2* binding sites (Fig. 6P). To ascertain whether *Satb2* can bind to any of these sites, we performed ChIP using an antibody against *Satb2* (raised in the laboratory of Y.K. and T.K.S.) and chromatin from the cortices of WT mice at P0. As a positive control, we tested previously published sequences in the *Ctip2* genomic locus for binding (Fig. 6Q) (9). As a negative control, we tested genomic sequences in a known gene desert region, which should show minimal or no interaction with *Satb2*. As expected, the negative control gene desert region showed minimal or no enrichment for *Satb2* binding, whereas MAR sequences from the *Ctip2* locus showed greater than sevenfold enrichment (when normalized to values observed in the gene desert region) (Fig. 6Q). We then used three primers specific to each MAR region in the *Tbr1* genomic locus and asked whether these showed enrichment for *Satb2* binding. All three sequences resulted in binding levels similar to that for the published *Ctip2* sites. These data suggest that *Satb2* can directly bind to the *Tbr1* locus, thereby positively regulating the expression of *Tbr1*.

Regulation of Callosal Projections in *Satb2* Mutant Neurons. Until this point we have focused on the genetic interactions that regulate the formation of subcerebral and subcortical connections by deep layer neurons. Here we consider the interactions that

Fig. 5. *Satb2* and *Ctip2* regulate *Tbr1* expression in a layer specific manner. (A–D) Immunostaining for *Tbr1* (green) and *Bhlhb5* (red) in P4 control cortex (A) reveals heavy staining in layer 6 and moderate staining in layer 5. A small fraction of cells in the upper layers are also *Tbr1*⁺. (B) *Satb2* conditional knockouts show reduced *Tbr1* in layers 6 and 5, and a loss of *Tbr1* in the upper layers. *Bhlhb5* expression is increased in the upper layers. (C) In *Ctip2* mutants, *Tbr1* staining increases in layers 6 and 5. (D) *Ctip2*^{-/-}; *Satb2*^{LacZ/LacZ} double knockouts at P0 show reduced *Tbr1* expression in layer 5 and increased *Bhlhb5* in the upper layers. (E and F) Immunostaining for *Tbr1* (green) and *Ctip2* (red) reveals an increase in *Tbr1* and a decrease in *Ctip2* expression in layer 5 of *Fezf2*^{PLAP/PLAP} mutants. *Ctip2* (red) but not *Tbr1* (green) expression is restored to control levels in layer 5 of *Fezf2*^{PLAP/PLAP};*Satb2*^{LacZ/Flox}; *Emx1-Cre* double knockouts (F). (A–F) Each panel is a composite of tiled confocal images to form the full figure. (Scale bar, 100 μm.) (G–I) Graphs depicting the percentage of *Tbr1*⁺ neurons in different layers of the genotypes under study. Error bars are average ± SEM (*n* = 3 different animals). Confidence levels were calculated using a *t* test (**P* < 0.05; ***P* < 0.01; ****P* < 0.005, relative to controls).

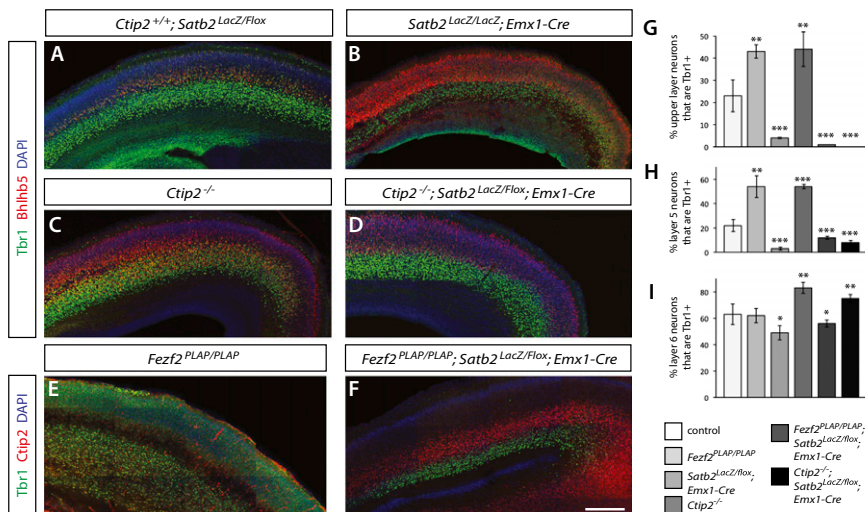
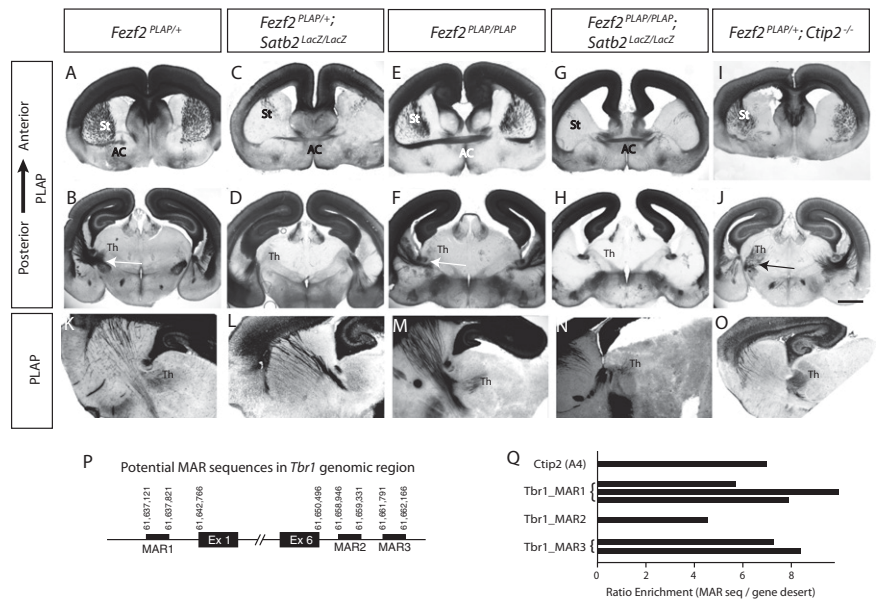


Fig. 6. Innervation of thalamus by PLAP⁺ axons correlates with *Tbr1* expression. (A, B, and K) PLAP⁺ control brains revealed robust PLAP staining in the striatum (st) and thalamus (Th). (C, D, and L) *Satb2* mutants show a reduction in PLAP⁺ axons traversing the striatum but almost no expression in the thalamus. (E, F, and M) *Fezf2* mutants show robust PLAP staining in the striatum, anterior commissure (AC), and thalamus. (G, H, and N) In *Fezf2*^{PLAP/PLAP}; *Satb2*^{LacZ/flox}; *Emx1-Cre* double mutants, PLAP staining is reduced in the striatum and thalamus but remains robust in the anterior commissure. (I, J, and O) Robust PLAP staining is observed in the striatum and thalamus of *Ctip2*^{-/-} mutants. (A–J) PLAP innervation using colorimetric substrate for alkaline phosphatase. (K–O) Immunostaining using an anti-PLAP antibody to visualize PLAP⁺ tracts. (Scale bar, 200 μ m.) All images are composites of tiled confocal images to show the entire section. (P) Genomic map representation of three MAR (matrix attachment regions) sequences identified in the *Tbr1* genomic locus. (Q) ChIP analysis of chromatin from P0 WT neonatal cortex immunoprecipitated with an antibody to *Satb2* using multiple primer sets targeting the *Tbr1* MAR regions. These experiments show comparable levels of enrichment relative to *Ctip2* A5 MAR [*Ctip2* 42/44 primer set (3)] region. Primers were normalized to a gene desert region. Each bar represents enrichment of the region using a distinct primer set designed to that region. Each primer set was tested at least three times in three independent samples.



mediate corticocortical connectivity as exemplified by the formation of axons that cross the CC, which we visualized using the *Satb2*^{LacZ} allele (9).

Satb2 mutants exhibit a failure of callosal development and the extension of β -gal⁺ axons to subcerebral targets, accompanied by a marked up-regulation of *Ctip2* staining throughout the cortex (9, 10), whereas *Fezf2* expression is unaltered. The ectopic expression of either *Ctip2* or *Fezf2* in WT upper layer neurons can divert their projections toward subcortical targets (8, 9), suggesting that the redirection of β -gal⁺ axons from callosal to subcerebral targets in *Satb2* mutants may be due to the up-regulation of *Ctip2*. We therefore set out to explore the genetic interactions between *Satb2* and *Ctip2* in the formation of cortical connectivity. If the upregulation of *Ctip2* is responsible for the alteration in axonal projections, then the loss of *Ctip2* in a *Satb2* mutant background should result in one of two possible outcomes: (i) the callosal projections of *Satb2* mutant neurons will be rescued and β -gal⁺ axons will again cross the midline, or (ii) a novel default fate (neither callosal nor subcortical) might be revealed.

In *Fezf2* and *Ctip2* single mutants [*Fezf2*^{PLAP/PLAP}; *Satb2*^{LacZ/+} (Fig. S2F) or *Ctip2*^{-/-}; *Satb2*^{LacZ/flox} (Fig. 1H and Fig. S2H)], β -gal⁺ axons from *Satb2*-expressing neurons cross the CC. As expected, in *Fezf2*^{PLAP/PLAP}; *Satb2*^{LacZ/LacZ} double knockouts, β -gal⁺ axons are absent from the CC and instead extend subcortically to the thalamus (Fig. S2K) and cerebral peduncle (Fig. S2L), similar to *Satb2* single mutants (Fig. S2C and D). These data confirm that *Fezf2* is not responsible for the fate change in *Satb2* mutant neurons.

LacZ staining of P0 brains from *Satb2* conditional mutants reveals that β -gal⁺ axons enter the pyramidal tract (Fig. 1B, F, and G), as expected. In contrast, β -gal⁺ axons are absent from the pyramidal tract of *Ctip2*^{-/-}; *Satb2*^{LacZ/flox}; *Emx1-Cre* double mutants (Fig. 1C), similar to control brains (Fig. 1A). Further, β -gal⁺ axons cross the CC (Fig. 1I) in these double mutants. These results suggest that the acquisition of *Ctip2* expression by neurons that lack *Satb2* is responsible, at least in part, for their failure to form callosal connections and the extension of β -gal⁺ axons to subcerebral targets (Fig. S1D). Interestingly, in *Ctip2*; *Satb2* double mutants, many β -gal⁺ neurons still continue to project subcortically to the striatum, cerebral peduncle, or thalamus (Fig. 1J, K, and L), although none reach the pyramidal tract

(Fig. 1L and M). Thus it seems that, without both *Satb2* and *Ctip2*, neurons that normally express *Satb2* may project callosally (owing to loss of *Ctip2*) or subcortically to the peduncle.

Overexpression of *Tbr1* Can Rescue Callosal Projections in *Satb2* Mutants.

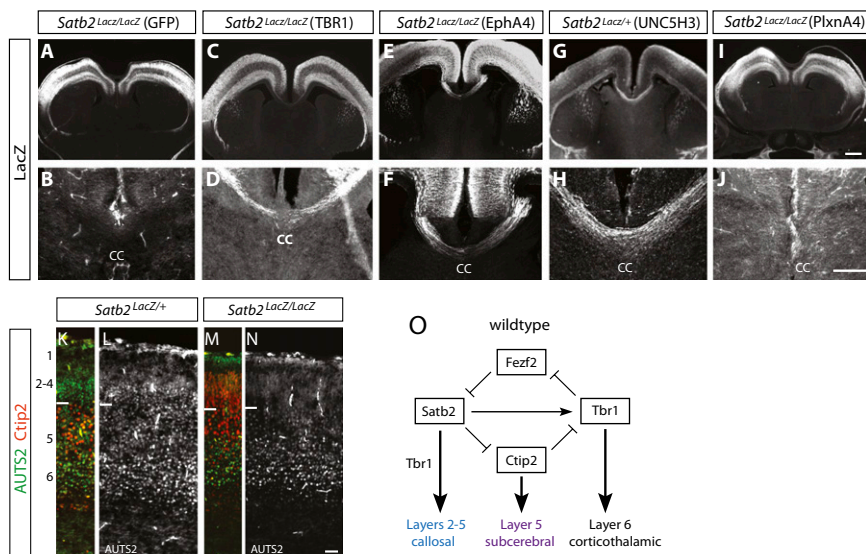
Tbr1 plays an important role in specifying the corticothalamic projections of layer 6 neurons (5, 7, 17), but upper layer neurons that normally express *Tbr1* do not project to the thalamus. This suggests that *Tbr1* might have an unexplored role in the upper layers. Indeed, in *Tbr1*^{-/-} mutant cortices, the axons of upper layer neurons fail to cross the CC and instead terminate in Probst bundles at the midline (17). Interestingly, restoring expression of *Tbr1* in the upper layers of *Tbr1*^{-/-} mutants did not direct those axons to the thalamus (7); instead they projected across the CC, consistent with the possibility that *Tbr1* in upper layer neurons plays a role in callosal connectivity. We therefore asked whether we could rescue the callosal defects in *Satb2*^{LacZ/LacZ} mutants by reintroducing *Tbr1* into the upper layers. Co-electroporation of expression constructs encoding *Tbr1* and GFP into E15.5 *Satb2*^{LacZ/LacZ} mutants does rescue the formation of callosal projections: β -gal⁺ axons cross the CC in all 10 electroporated mutant embryos (Fig. 7C and D), suggesting that expression of *Tbr1* can compensate for the loss of *Satb2*. This defines a new function for *Tbr1* and places *Tbr1* genetically downstream of *Satb2* in callosal neuron specification. Thus, in the developing cortex, *Tbr1* has a dual function, first specifying layer 6 corticothalamic neurons and later in callosal connectivity.

Loss of *Tbr1* Expression in *Satb2* Mutants Coincides with a Loss of *Auts2*.

Tbr1 binds to and directly activates the expression of *Auts2*, a gene expressed in frontal cortex that has been linked to autism and mental retardation (18). The functional significance of this relationship has been puzzling because *Tbr1* regulates corticothalamic identity, and there have been no reports of defects in corticothalamic tracts in autistic patients. However, imaging studies in patients with autism have revealed defects in callosal tracts (2, 19–26). A recent publication highlights a deficit in long-range connections (such as callosal connections) and excess of short-range cortical connections in patients with autism spectrum disorder (27).

Auts2, like *Tbr1*, is expressed in both the deep and upper layers of the cortex (Fig. 7K and L). Because *Tbr1* regulates

Fig. 7. *Tbr1*, *EphA4*, and *Unc5h3* are downstream targets of *Satb2* and can direct callosal projections. β -Gal⁺ axons fail to cross the CC in *Satb2*^{LacZ/LacZ} mutants electroporated with either a *GFP* control construct (A and B) or a *PlxnA4* expression construct together with *GFP* (I and J). β -Gal⁺ axons cross the CC in *Satb2* mutants electroporated with *TBR1-IRES-GFP* (C and D), *EphA4* and *GFP* (E and F), or *Unc5H3* and *GFP* (G and H). E and F are composites of tiled images to form the full figure. (Scale bar, 100 μ m.) (K–N) *Auts2* expression is lost in the upper layers of *Satb2* mutants. (K and L) *Auts2* protein (green in K, white in L) is expressed in both the upper and deep layers of control *Satb2*^{LacZ/+} brains at P0. *Ctip2* expression is shown in red. (M and N) *Auts2* expression is maintained in layer 6 of *Satb2* mutants but is down-regulated in the upper layers. (Scale bar, 50 μ m.) (O) Model of genetic interactions between *Fezf2*, *Ctip2*, *Satb2*, and *Tbr1* in wild type cortex. *Fezf2* expression in layer 5 neurons represses *Tbr1* and *Satb2*, which repress corticothalamic and callosal fates, respectively. The repression of *Satb2* enables expression of *Ctip2* and *Bhlhb5*, which are required for the specification and execution of a subcerebral identity. In *Satb2* expressing neurons, *Ctip2* is repressed, leading to a repression of subcerebral identity and acquisition of callosal and corticocortical axonal projections.



Auts2, we investigated whether the loss of *Tbr1* expression in upper layer neurons in *Satb2*^{LacZ/LacZ} mutants coincides with changes in the expression of *Auts2*. We observed a striking loss of *Auts2* expression in the upper layers of *Satb2* mutants (Fig. 7 M and N), similar to the loss of *Tbr1* in *Satb2* mutants (Fig. 5B); there was no change in *Auts2* expression in layers 5 or 6 (Fig. 7 M and N) relative to controls (Fig. 7 K and L). These data are consistent with the possibility that *Satb2* regulates the expression of *Tbr1*, which in turn is required for *Auts2* expression in callosal projection neurons. These results may have implications for the etiology of autism.

Expression of *EphA4* and *Unc5H3* Restores Callosal Projections in *Satb2* Mutants. Previously we identified several genes that show altered expression in *Satb2*^{LacZ/LacZ} mutants (9). In particular, three axonal guidance molecules (*EphA4*, *PlxnA4*, and *Unc5H3*) are down-regulated in upper layers of mice lacking *Satb2*. Prior studies have implicated Ephs and ephrins in callosal development (13, 28, 29). *EphA4* is normally expressed in upper layer callosal neurons and the glial wedge (28). In *Satb2* mutants, *EphA4* expression is lost in cortical neurons, but expression in the glial wedge is maintained (9). *Unc5H3* mutants have no reported callosal deficiencies (13), but mice lacking *Netrin*, a ligand for *Unc5H3*, lack both the CC and the anterior commissure (29, 30). To test the hypothesis that one or more of these genes is required for the proper guidance of callosal axons to their destinations, we attempted to rescue the formation of callosal projections in *Satb2* mutants by reintroducing the expression of individual axon guidance molecules into upper layer neurons. In utero electroporation of *PlxnA4* failed to rescue callosal projections (Fig. 7 I and J) in *Satb2*^{LacZ/LacZ} mutants, but electroporation of *EphA4* (Fig. 7 E and F) or *Unc5H3* (Fig. 7 G and H) resulted in the extension of β -gal⁺ axons across the CC. These results suggest that *EphA4* and *Unc5H3* are critical downstream targets of *Satb2* in callosal fate specification.

Discussion

Our data suggest that cortical projection neurons actively repress alternate fates to promote appropriate fate choices during development (Fig. 7O). When specific repressive interactions are removed, alternative fates are executed (Fig. S1). Whereas *Tbr1*, *Ctip2*, and *Satb2* are expressed in postmitotic neurons, *Fezf2* is expressed in cycling cortical progenitors from very early stages of corticogenesis (11). Loss of *Fezf2* is critical for the specification of the subcerebral projections of layer 5 neurons, as evidenced by

the loss of corticospinal projections in *Fezf2* mutants (11, 14). During the earliest stages of corticogenesis, *Sox5* expression in subplate and layer 6 neurons represses the expression of *Fezf2* (and consequently that of *Ctip2*) (15, 16). This likely promotes the expression of *Tbr1* in layer 6 neurons. *Tbr1* binds to and represses the *Fezf2* genomic locus (5, 7), thereby suppressing a subcerebral fate and promoting the formation of corticothalamic projections from layer 6. *Sox5* expression is down-regulated early in layer 5 neurons (15, 16), leading to a derepression of *Fezf2*, which consequently leads to a repression of *Satb2*. The effect of this is threefold. First, there are no intracellular triggers to promote a callosal fate. Second, the absence of *Satb2*-mediated repression of *Ctip2* and *Bhlhb5* leads to the continued expression of these genes and the extension of subcortical axons. (Interestingly, although *Bhlhb5* expression in *Satb2* mutants at E18 does not differ from that in controls, expression at P4 is significantly increased in *Satb2* mutants. This suggests that *Satb2* is required for the normal down-regulation of *Bhlhb5* expression during early prenatal development, and that the sustained expression of *Bhlhb5* in *Satb2* mutants might be important in executing or maintaining the new subcerebral fate of these neurons.) Third, our data indicate that the absence of *Satb2*-mediated activation of *Tbr1* suppresses corticothalamic projections. Thus, *Fezf2*-expressing layer 5 neurons extend their axons subcerebrally.

We hypothesize that during production of the upper layers, the absence of *Fezf2* in cortical progenitors allows their daughters to express *Satb2*, which in turn promotes a callosal identity (in part, surprisingly, by activating *Tbr1* in upper layer neurons). Simultaneously, activation of *Satb2* results in the repression of *Ctip2* and *Bhlhb5*, ensuring that executors of subcortical identity remain inactive in callosal neurons. Thus, each phase of corticogenesis and neuronal fate specification deploys an active repression of previous fates and a promotion of the appropriate layer-specific projection fate (see *SI Discussion* for further details).

Tbr1 seems to play distinct roles at different stages of cortical development. At early stages, *Tbr1* promotes a frontal identity while suppressing caudal identity (4). During the formation of layer 6, *Tbr1* plays an essential role in specifying the fates and projection patterns of corticothalamic neurons (4, 5, 7, 17). Interestingly, although corticothalamic projections are decreased in *Tbr1* mutants and increased in *Fezf2* mutants (which show an up-regulation of *Tbr1*), these alterations in projections are incomplete: there are still some corticothalamic axons in *Tbr1* mutants, and *Fezf2* mutant neurons do not completely convert to

corticothalamic identity, suggesting that *Tbr1* cannot be the sole specifier of a corticothalamic fate.

In addition, we found that *Satb2* and *Ctip2* dynamically regulate the expression of *Tbr1* in a layer dependent manner. *Satb2* seems to promote expression of *Tbr1*, whereas *Ctip2* represses *Tbr1* expression. This complex bidirectional regulation might explain why we observe a partial rescue of callosal axon targeting in *Ctip2;Satb2* double mutants (Fig. S1F). In these animals, *Tbr1* expression in layer 5 neurons is partially rescued (relative to *Satb2* single mutants) and might account for the partial rescue of callosal projections in these animals. In the upper layers, *Tbr1* seems to play a unique role in promoting the formation of callosal projections, which may explain why *Tbr1* mutants display callosal agenesis (17). This role for *Tbr1* in callosal development is also intriguing in the context of autism. Autistic patients seem to have callosal abnormalities (19–26), and in this context it is relevant that *Auts2*, a gene associated with autism, is regulated by *Tbr1*, which in turn is regulated by *Satb2*, a callosal fate specification gene. Recent studies suggest that a mutation in *CAV1/2* (an L-type calcium channel) that is associated with Timothy syndrome, a form of autism, results in lower numbers of *Satb2*-expressing cells and an increase in *Ctip2*-expressing cells (31). The authors suggest that the reduction in callosal neurons in Timothy syndrome is consistent with the emerging view that autism spectrum disorders arise from defects in connectivity between cortical areas (31).

The role of axon guidance molecules, specifically Ephrins and their receptors, in directing callosal neurons has been studied extensively using genetic knockouts. Although the loss of single genes does not result in dramatic callosal abnormalities, double knockouts of various genotypes do compromise callosal development, suggesting that there is redundancy built into the system. Indeed, it is interesting to note that although restoring *EphA4* expression in *Satb2* mutants rescued callosal projections, *EphA4* knockout mice fail to display callosal defects (28). However,

multiple EphB receptors (B1, B2, and B3) and ligands (ephrinB1, B2, and B3) are expressed in callosal fibers and midline guidepost cells, respectively, and it is likely that their functions are redundant. Restoring expression of *Unc5h3* also rescued callosal projections in *Satb2* mutants. *Unc5H3* is normally expressed throughout the cortical plate during development, and no callosal defects have been observed in *Unc5h3^{rem}* null mice, although these mice display subcortical defects in CST development (13). Our findings suggest an unexpected role for this receptor in callosal development.

Methods

Animals. *Satb2^{LacZ/+}*, *Fezf2^{PLAP/+}*, and *Ctip2^{+/-}* animals were mated to generate appropriate double knockouts. Details of generation of the conditional *Satb2* single and double mutants are described in *SI Methods*.

Immunohistochemistry. Standard immunohistochemistry techniques were used. Details of antibodies used in the study are listed in *Table S1*. PLAP staining was performed as described previously (11).

In Utero Electroporation: Methods are as described in previous work (8).

ChIP. Experiments were performed as described earlier (9) using a rabbit anti-*Satb2* antibody. MAR sequence predictions were based on www.genomatix.de. For primer sequences, refer to *Table S2*.

ACKNOWLEDGMENTS. We thank Bin Chen and William McKenna (University of California, Santa Cruz) for sharing reagents; Geetu Tuteja, Lee Shoa Long Clarke, and Bruce Schaar (Stanford University) for help and advice with ChIP experiments; Jeffrey Macklis (Harvard University) for *Ctip2* mutant mice; Avraham Yaron (Weizmann Institute) for *EphA4* and *PlxnA4* expression constructs; and Robert Nechanitzky and Thomas Manke (laboratory of R.G.) for helping with in silico analyses of *Satb2* binding sites. This study was funded by National Institutes of Health Grants EY08411 (to S.K.M.) and K99 MH086720 (to K.S.).

- Arlotta P, et al. (2005) Neuronal subtype-specific genes that control corticospinal motor neuron development in vivo. *Neuron* 45(2):207–221.
- Koester SE, O'Leary DD (1993) Connectional distinction between callosal and subcortically projecting cortical neurons is determined prior to axon extension. *Dev Biol* 160(1):1–14.
- Leone DP, Srinivasan K, Chen B, Alcamo E, McConnell SK (2008) The determination of projection neuron identity in the developing cerebral cortex. *Curr Opin Neurobiol* 18(1):28–35.
- Bedogni F, et al. (2010) *Tbr1* regulates regional and laminar identity of postmitotic neurons in developing neocortex. *Proc Natl Acad Sci USA* 107(29):13129–13134.
- Han W, et al. (2011) *TBR1* directly represses *Fezf2* to control the laminar origin and development of the corticospinal tract. *Proc Natl Acad Sci USA* 108(7):3041–3046.
- Hevner RF, Miyashita-Lin E, Rubenstein JL (2002) Cortical and thalamic axon pathfinding defects in *Tbr1*, *Gbx2*, and *Pax6* mutant mice: evidence that cortical and thalamic axons interact and guide each other. *J Comp Neurol* 447(1):8–17.
- McKenna WL, et al. (2011) *Tbr1* and *Fezf2* regulate alternate corticofugal neuronal identities during neocortical development. *J Neurosci* 31(2):549–564.
- Chen B, et al. (2008) The *Fezf2-Ctip2* genetic pathway regulates the fate choice of subcortical projection neurons in the developing cerebral cortex. *Proc Natl Acad Sci USA* 105(32):11382–11387.
- Alcamo EA, et al. (2008) *Satb2* regulates callosal projection neuron identity in the developing cerebral cortex. *Neuron* 57(3):364–377.
- Britanova O, et al. (2008) *Satb2* is a postmitotic determinant for upper-layer neuron specification in the neocortex. *Neuron* 57(3):378–392.
- Chen B, Schaevitz LR, McConnell SK (2005) *Fezl* regulates the differentiation and axon targeting of layer 5 subcortical projection neurons in cerebral cortex. *Proc Natl Acad Sci USA* 102(47):17184–17189.
- Joshi PS, et al. (2008) *Bhlhb5* regulates the postmitotic acquisition of area identities in layers II–V of the developing neocortex. *Neuron* 60(2):258–272.
- Finger JH, et al. (2002) The netrin 1 receptors *Unc5h3* and *Dcc* are necessary at multiple choice points for the guidance of corticospinal tract axons. *J Neurosci* 22(23):10346–10356.
- Molyneaux BJ, Arlotta P, Hirata T, Hibi M, Macklis JD (2005) *Fezl* is required for the birth and specification of corticospinal motor neurons. *Neuron* 47(6):817–831.
- Kwan KY, et al. (2008) *SOX5* postmitotically regulates migration, postmigratory differentiation, and projections of subplate and deep-layer neocortical neurons. *Proc Natl Acad Sci USA* 105(41):16021–16026.
- Lai T, et al. (2008) *SOX5* controls the sequential generation of distinct corticofugal neuron subtypes. *Neuron* 57(2):232–247.
- Hevner RF, et al. (2001) *Tbr1* regulates differentiation of the preplate and layer 6. *Neuron* 29(2):353–366.
- Bedogni F, et al. (2010) Autism susceptibility candidate 2 (*Auts2*) encodes a nuclear protein expressed in developing brain regions implicated in autism neuropathology. *Gene Expr Patterns* 10(1):9–15.
- Anderson JS, et al. (2011) Decreased interhemispheric functional connectivity in autism. *Cereb Cortex* 21(5):1134–1146.
- Elia J, et al. (2010) Rare structural variants found in attention-deficit hyperactivity disorder are preferentially associated with neurodevelopmental genes. *Mol Psychiatry* 15(6):637–646.
- Freitag CM, et al. (2009) Total brain volume and corpus callosum size in medication-naïve adolescents and young adults with autism spectrum disorder. *Biol Psychiatry* 66(4):316–319.
- Jou RJ, et al. (2011) Diffusion tensor imaging in autism spectrum disorders: Preliminary evidence of abnormal neural connectivity. *Aust N Z J Psychiatry* 45(2):153–162.
- Lo YC, et al. (2011) The loss of asymmetry and reduced interhemispheric connectivity in adolescents with autism: A study using diffusion spectrum imaging tractography. *Psychiatry Res* 192(1):60–66.
- Mengotti P, et al. (2011) Altered white matter integrity and development in children with autism: A combined voxel-based morphometry and diffusion imaging study. *Brain Res Bull* 84(2):189–195.
- Shukla DK, Keehn B, Müller RA (2011) Tract-specific analyses of diffusion tensor imaging show widespread white matter compromise in autism spectrum disorder. *J Child Psychol Psychiatry* 52(3):286–295.
- Thomas C, Humphreys K, Jung KJ, Minshew N, Behrmann M (2011) The anatomy of the callosal and visual-association pathways in high-functioning autism: a DTI tractography study. *Cortex* 47(7):863–873.
- Barttfeld P, et al. (2011) A big-world network in ASD: Dynamical connectivity analysis reflects a deficit in long-range connections and an excess of short-range connections. *Neuropsychologia* 49(2):254–263.
- Mendes SW, Henkemeyer M, Liebl DJ (2006) Multiple Eph receptors and B-class ephrins regulate midline crossing of corpus callosum fibers in the developing mouse forebrain. *J Neurosci* 26(3):882–892.
- Serafini T, et al. (1996) *Netrin-1* is required for commissural axon guidance in the developing vertebrate nervous system. *Cell* 87(6):1001–1014.
- Métin C, Deléglise D, Serafini T, Kennedy TE, Tessier-Lavigne M (1997) A role for *netrin-1* in the guidance of cortical efferents. *Development* 124(24):5063–5074.
- Paşca SP, et al. (2011) Using iPSC-derived neurons to uncover cellular phenotypes associated with Timothy syndrome. *Nat Med* 17(12):1657–1662.

Supporting Information

Srinivasan et al. 10.1073/pnas.1216793109

SI Methods

Generation of Double Mutants. Double mutant pups die within 2 h of birth, and all analyses shown here were performed on postnatal day (P) 0 pups collected just after birth. Animals were genotyped as described previously (1, 2). The *Satb2* conditional allele was generated in R.G.'s laboratory. *Satb2*^{flax/flax} mice were first bred to *Satb2*^{LacZ/+} mice to generate *Satb2*^{LacZ/flax} animals. These animals were then bred to *Satb2*^{LacZ/+}; *Emx1-Cre* mice to generate *Satb2* conditional mutants that carry a LacZ allele, which enabled us to visualize the axons of neurons that normally express *Satb2*. During the generation of *Satb2*; *Fezf2* double knockouts, *Fezf2*^{PLAP/+}; *Satb2*^{LacZ/+} double heterozygous mice were crossed to Swiss Webster wild type animals for six to eight generations to eliminate lethality arising owing to strain differences between the parent *Fezf2*^{PLAP/+} and *Satb2*^{LacZ/+} animals. During this process we were able to generate *Fezf2* mutant animals that had an intact corpus callosum, unlike the original parent strain of *Fezf2* mutants. The presence of a corpus callosum in the new *Fezf2* mutants enabled us to visualize PLAP⁺ fibers crossing the midline in these animals.

Quantitation of Cell Type Markers. To quantitate changes in the expression of *Ctip2*, *Bhlhb5*, and *Tbr1*, the boundaries of layers 6, 5, and upper layers 2/3 were first defined using a panel of layer-specific markers (including *Sox5*, *Tle4*, *Fog2*, *Brn2*, and *Lmo4*) in each genotype. Confocal images in 40× field of view were acquired on a Zeiss LSM 510 meta confocal microscope. Epi-fluorescent images were acquired on a Nikon 80i microscope with a Hamamatsu Orca ER camera. Images were postprocessed

using ImageJ and Adobe Photoshop CS3. We then counted the fraction of cells that expressed the protein of interest within each layer, including counts from three sections each from anterior to posterior cortex from at least three animals. Data are presented as averages ± SEM. *P* values were calculated using the *t* test function in Microsoft Excel.

SI Discussion

“Derepression” also plays a crucial role in spinal cord development, where the sequential disinhibition of key executor genes promotes specific projection identities (3). However, in the spinal cord, a gradient of Sonic hedgehog (Shh) generates a spatial parcellation of progenitor cells that express distinct combinations of transcription factors, which results in the generation of specific motor neuron subtypes at roughly the same time (3). In the cortex, birthdate and timing of mitotic exit play critical roles in regulating the factors that specify cell identity (4, 5). The expression of *Fezf2* by progenitors in the ventricular zone at early times during development likely biases deep layer neurons toward subcortical projection fates, and the later expression of genes such as *Tbr1* and *Ctip2* enables neurons to execute specific identities. In callosal neurons, we see a similar pattern in which *Satb2* specifies callosal identity, which is executed by genes such as *Tbr1* and possibly refined by genes such as *Cpne4* and *Btg1* (6), which are expressed by subsets of callosal neurons. It is interesting that although callosal neurons in layer 2/3 seem to be evolutionarily more recent than the subcortically projecting cells, the underlying mechanism of repression followed by derepression of key target genes is similar to that observed in deep layer neurons.

1. Chen B, et al. (2008) The *Fezf2-Ctip2* genetic pathway regulates the fate choice of subcortical projection neurons in the developing cerebral cortex. *Proc Natl Acad Sci USA* 105(32):11382–11387.
2. Alcamo EA, et al. (2008) *Satb2* regulates callosal projection neuron identity in the developing cerebral cortex. *Neuron* 57(3):364–377.
3. Lee SK, Pfaff SL (2001) Transcriptional networks regulating neuronal identity in the developing spinal cord. *Nat Neurosci* 4(Suppl):1183–1191.

4. McConnell SK (1992) The control of neuronal identity in the developing cerebral cortex. *Curr Opin Neurobiol* 2(1):23–27.
5. McConnell SK (1991) Cell cycle dependence of laminar determination in developing neocortex. *Science* 254(5029):282–285.
6. Fame RM, MacDonald JL, Macklis JD (2011) Development, specification, and diversity of callosal projection neurons. *Trends Neurosci* 34(1):41–50.

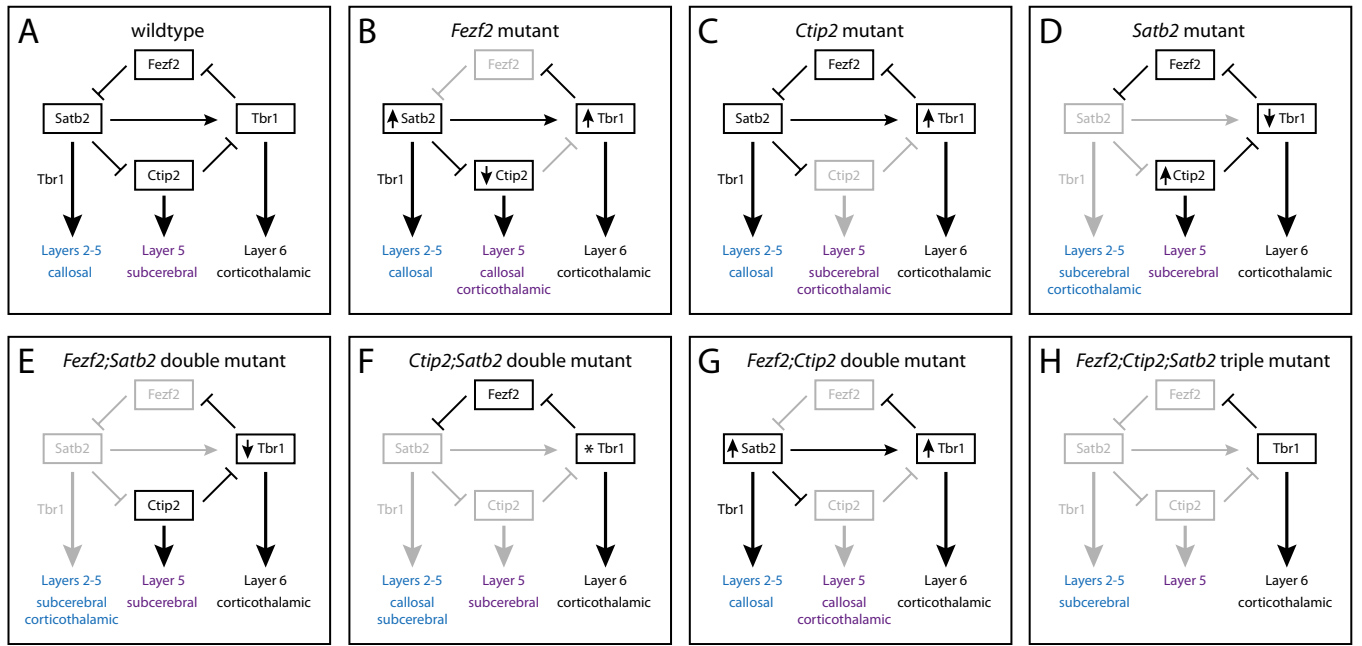


Fig. S1. Model of the genetic interactions that confer cell fate specification in cortical projection neurons. Genetic interactions between *Fezf2*, *Ctip2*, *Satb2*, and *Tbr1* are represented for single and double mutants. Cells that normally express *Fezf2* are marked by PLAP (purple), and *Satb2*-expressing cells are marked by β -gal (blue). Gray boxes represent genes that are absent in the genotype. Final projection identities in *Fezf2*, *Satb2*, and *Tbr1*-expressing neurons are shown at the bottom of each cell type. (A) In wild type cortex, *Fezf2* expression in layer 5 neurons represses *Tbr1* and *Satb2*, which represent corticothalamic and callosal fates, respectively. The repression of *Satb2* enables expression of *Ctip2* and *Bhlhb5*, which are required for the specification and execution of a subcerebral identity. In *Satb2*-expressing neurons, *Ctip2* is repressed, leading to a repression of subcerebral identity and acquisition of callosal and corticocortical axonal projections. (B) *Fezf2* mutant neurons fail to repress both *Satb2* and *Tbr1*, resulting in PLAP⁺ axons that cross the CC and/or innervate the thalamus inappropriately, as denoted by the shift of layer 5 neurons to callosal and corticothalamic fates. (C) *Ctip2* mutant neurons continue to express *Fezf2* and thus project subcortically. However, without *Ctip2*, these axons are unable to extend past the pons. Repression of *Tbr1* is lost, leading to inappropriate *Tbr1* expression in *Ctip2* mutant cells and increased corticothalamic innervation. (D) *Satb2* mutant neurons fail to repress *Ctip2* and project subcerebrally toward the pons. β -Gal⁺ axons also project inappropriately to the thalamus, suggesting that in callosal neurons, *Satb2* normally represses gene(s) that promote a corticothalamic fate. (E) In *Fezf2*;*Satb2* double mutants, *Ctip2* expression is restored in layer 5, enabling PLAP⁺ neurons to extend subcerebral axons. β -Gal⁺ neurons, which normally express *Satb2*, project axons inappropriately to subcerebral destinations because of up-regulating *Ctip2*, and to the thalamus because of the up-regulation of an as-yet unidentified gene. Because *Tbr1* expression in layer 6 neurons is unaffected, they continue to project to thalamus. (F) β -Gal⁺ axons in *Ctip2*;*Satb2* double mutants show a partial rescue: a fraction project normally across the CC, but others project inappropriately to subcerebral targets. PLAP⁺ axons of *Fezf2*-expressing layer 5 neurons project subcortically but do not extend past the pons because of a loss of *Ctip2*. (G) In *Fezf2*;*Ctip2* double mutants, PLAP⁺ neurons acquire *Satb2* expression and project callosally and/or acquire *Tbr1* expression and project to thalamus. (H) In the absence of *Fezf2*, *Ctip2*, and *Satb2*, only *Tbr1* expression in layer 6 is maintained, and those axons extend to thalamus. β -Gal⁺ axons project inappropriately to the thalamus or sub-cerebrally, although their axons fail to extend past the cerebral peduncle. PLAP⁺ axons of layer 5 neurons are unable to extend past the white matter without *Fezf2* or *Ctip2*.

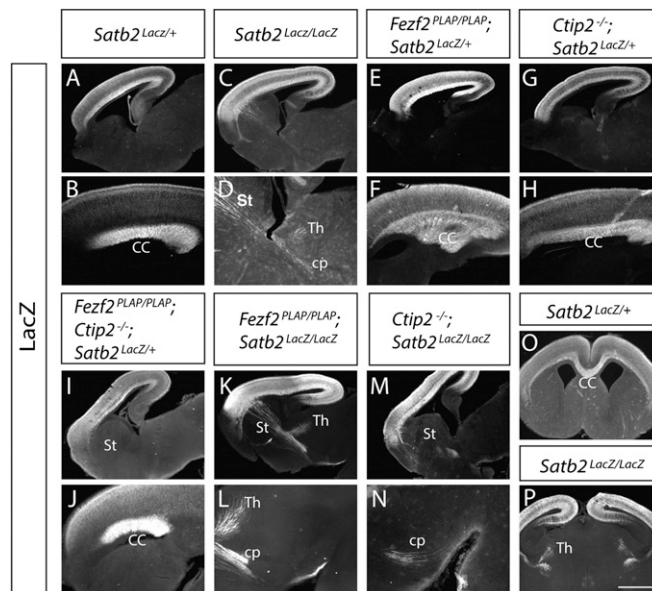


Fig. S2. Aberrant axon targeting of *Satb2*-expressing neurons visualized by β -galactosidase (β -gal) immunostaining in single and double mutants of *Satb2*, *Fezf2*, and *Ctip2*. (A and B) The β -gal⁺ axons of neurons that express *Satb2* are observed in the corpus callosum (CC) at P0. (C and D) Callosal neurons lacking *Satb2* extend axons through the striatum (St) and into the thalamus (Th) and cerebral peduncle (cp). (E–J) β -Gal⁺ axons from *Satb2*-expressing neurons project across the CC at P0 in *Fezf2* mutants (E and F), *Ctip2* mutants (G and H), and *Fezf2*^{PLAP/PLAP};*Ctip2*^{-/-} double mutants (I and J). (K and L) β -Gal⁺ axons in *Satb2*^{LacZ/LacZ}; *Fezf2*^{PLAP/PLAP} double mutants extend through the striatum (St) and into the thalamus (Th) and cerebral peduncle (cp). (M and N) β -Gal⁺ axons in *Satb2*^{LacZ/LacZ}; *Ctip2*^{-/-} double mutants subcerebrally to the striatum and cerebral peduncle. (O) Coronal view of β -gal⁺ projecting across the corpus callosum in control mice. (P) Coronal view of in *Satb2* mutants, in which β -gal⁺ axons project inappropriately to the thalamus. (Scale bar, 200 μ m).

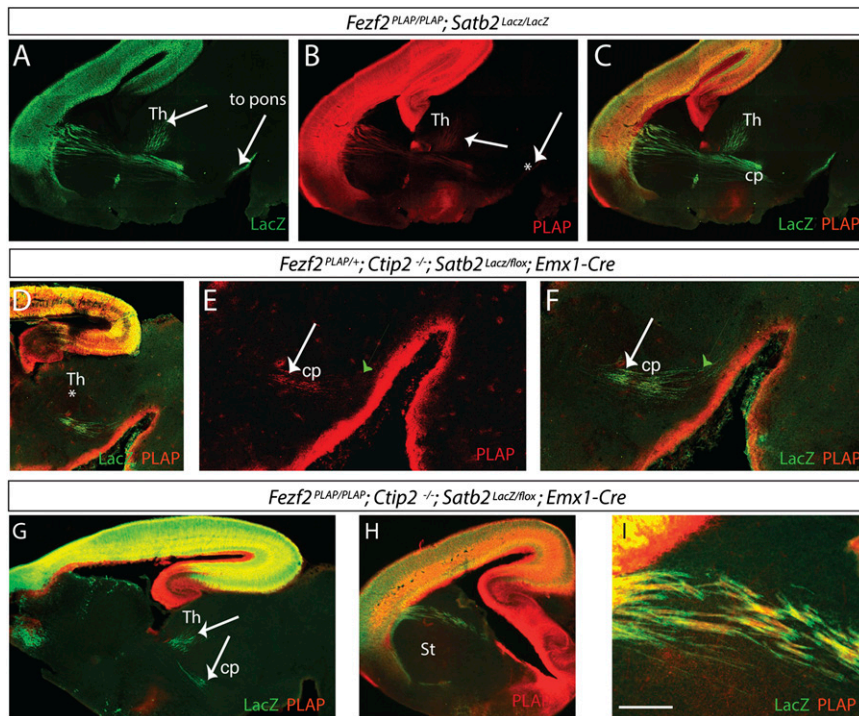


Fig. S3. Aberrant axon targeting of *Fezf2*-expressing neurons (visualized by PLAP staining) and *Satb2*-expressing neurons (visualized by β -gal staining) in double and triple mutants of *Satb2*, *Fezf2*, and *Ctip2*. (A–C) Immunostaining for β -gal (green) and PLAP (red) in *Fezf2*^{PLAP/PLAP};*Satb2*^{LacZ/LacZ} double mutants reveals robust β -gal⁺ and PLAP⁺ axons extending through the striatum, thalamus (Th), and along the cerebral peduncle (cp), heading toward the pons. Each panel is a composite of tiled images to form the full figure. (D–F) Immunostaining for β -gal (green) and PLAP (red) in *Ctip2*^{-/-};*Satb2*^{LacZ/lox};*Emx1-Cre* double mutants (heterozygous for *Fezf2*^{PLAP/+}) reveals β -gal⁺ and PLAP⁺ axons in the cerebral peduncle (cp) but absent from the thalamus (Th). (G and H) Immunostaining for β -gal (green) and PLAP (red) in *Fezf2*^{PLAP/PLAP};*Ctip2*^{-/-};*Satb2*^{LacZ/lox};*Emx1-Cre* triple mutants reveals that β -gal⁺ axons extend into the thalamus (Th) and cerebral peduncle (cp). PLAP⁺ axons, however, fail to project past the striatum. (I) Axons positive for both β -gal (green) and PLAP (red) are seen medial to the striatum in anterior sections. (Scale bar, 200 μ m).

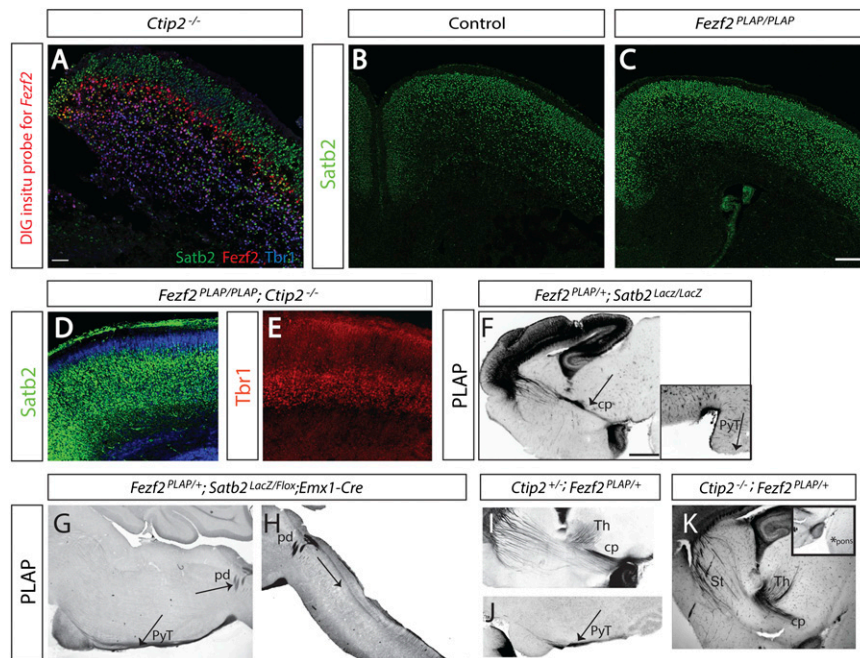


Fig. S4. (A) In situ hybridization using a digoxigenin-labeled probe against *Fezf2* in *Ctip2*^{-/-} mutants shows no change in *Fezf2* mRNA expression in these mutants. *Tbr1* immunostaining (blue) shows an increase of *Tbr1* expression in layers 6 and 5. *Satb2* immunostaining is visualized in green. (B and C) *Satb2* immunostaining (green) in control and *Fezf2*^{PLAP/PLAP} brains confirms previous reports of the expansion of *Satb2* expression in layer 5. (Scale bar, 50 μ m.) (D and E) In *Ctip2*^{-/-}; *Fezf2*^{PLAP/PLAP} double mutants, we observe an expansion of *Satb2* immunostaining (D) and normal *Tbr1* staining in layer 6 (E). (F) PLAP staining in the *Satb2*^{LacZ/LacZ} mutant cortex at embryonic day 18 reveals only a narrow band of PLAP⁺ axons that extend past the striatum and no PLAP⁺ axons at the level of the pyramidal tract (PyT in Inset). (G and H) In *Fezf2*^{PLAP/+}; *Satb2*^{LacZ/Flox}; *Emx1-Cre* mutant brains at P4, PLAP⁺ axons extend along the pyramidal tract and reach the pyramidal decussation (pd) but fail to extend past the decussation into the spinal cord (arrow in H). (I and J) PLAP staining at P0 in *Ctip2*^{+/-}; *Fezf2*^{PLAP/+} mice reveals that PLAP⁺ axons project normally into the pyramidal tract (PyT). I is a composite of tiled images to form the full figure. (K and L) In *Ctip2*^{-/-} mutants, PLAP-stained axons appear disorganized as they traverse the striatum (K) and are absent at the level of pons (L). (Scale bar, 200 μ m.)

Table S1. Antibodies (including source and dilution) used to detect proteins of interest

Mouse anti-Satb2	Abcam, 1:200
Rabbit anti-Ctip2	Abcam, 1:200
Rabbit anti-GFP	Invitrogen, 1:500
Chicken anti-LacZ	Abcam, 1:200
Rabbit anti-AUTS2	Sigma, 1:200 (citrate treatment)
Rabbit anti-Tbr1	Abcam, 1:200
Chicken anti-GFP	Abcam, 1:200
Goat anti-Bhlhb5	SCBT, 1:200
Rabbit anti-Sox5	Abcam, 1:200

Table S2. Primer sequences used to detect MAR sequences present in *Tbr1*

TBR1-MAR1-AMP1A	GGACCTTCTCCTCGAATGTG
TBR1-MAR1-AMP1B	CAGGTTAAAAAATTGAACCTAAAAATTGC
TBR1-MAR1-AMP2A	CAATTTTAAGTTCAATTTTAACTGT
TBR1-MAR1-AMP2B	TTTTAATGTCAGATGATGCTTTATTTA
TBR1-MAR1-AMP3A	TTGCAATAGTAAGGTTATATGGAATT
TBR1-MAR1-AMP3B	CGAACACATTGTTACATTCTTG
TBR1-MAR2-AMP1A	GTGTGTGTGTGTACCCGTC
TBR1-MAR2-AMP1B	CCATGGCATCAACTTCAAAA
TBR1-MAR2-AMP2A	GATGCCATGGGCATTTAGAA
TBR1-MAR2-AMP2B	GAAAAGTAAGGGCAGGCAAA
TBR1-MAR3-AMP1A	TGTTCCCAGATTGAAAATGGT
TBR1-MAR3-AMP1B	CAAAAACAGGAAGTGCTCAG
TBR1-MAR3-AMP2A	CTGAGGCACCTTCTGTTTTG
TBR1-MAR3-AMP2B	GATGCTTTGGTTTGCCAAG